



HAL
open science

**Accepted Manuscript An Improved Static-Analytic
Apparatus for Vapor-Liquid Equilibrium (PTxy)
Measurement Using Modified In-situ Samplers**

Fan, Zhang, Pascal Théveneau, Elise El Ahmar, Xavier Canet, Chien-Bin Soo,
Christophe Coquelet

► **To cite this version:**

Fan, Zhang, Pascal Théveneau, Elise El Ahmar, Xavier Canet, Chien-Bin Soo, et al.. Accepted Manuscript An Improved Static-Analytic Apparatus for Vapor-Liquid Equilibrium (PTxy) Measurement Using Modified In-situ Samplers. Fluid Phase Equilibria, 2015, 10.1016/j.fluid.2015.10.041 . hal-01228405v1

HAL Id: hal-01228405

<https://minesparis-psl.hal.science/hal-01228405v1>

Submitted on 13 Nov 2015 (v1), last revised 19 Jan 2016 (v2)

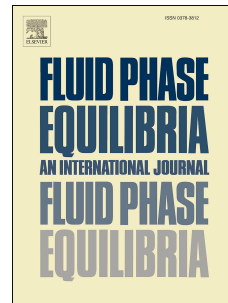
HAL is a multi-disciplinary open access archive for the deposit and dissemination of scientific research documents, whether they are published or not. The documents may come from teaching and research institutions in France or abroad, or from public or private research centers.

L'archive ouverte pluridisciplinaire **HAL**, est destinée au dépôt et à la diffusion de documents scientifiques de niveau recherche, publiés ou non, émanant des établissements d'enseignement et de recherche français ou étrangers, des laboratoires publics ou privés.

Accepted Manuscript

An Improved Static-Analytic Apparatus for Vapor-Liquid Equilibrium (PT_{xy}) Measurement Using Modified In-situ Samplers

Fan Zhang, Pascal Théveneau, Elise El Ahmar, Xavier Canet, Chien-Bin Soo, Christophe Coquelet



PII: S0378-3812(15)30200-4

DOI: [10.1016/j.fluid.2015.10.041](https://doi.org/10.1016/j.fluid.2015.10.041)

Reference: FLUID 10838

To appear in: *Fluid Phase Equilibria*

Received Date: 8 September 2015

Revised Date: 26 October 2015

Accepted Date: 27 October 2015

Please cite this article as: F. Zhang, P. Théveneau, E. El Ahmar, X. Canet, C.-B. Soo, C. Coquelet, An Improved Static-Analytic Apparatus for Vapor-Liquid Equilibrium (PT_{xy}) Measurement Using Modified In-situ Samplers, *Fluid Phase Equilibria* (2015), doi: 10.1016/j.fluid.2015.10.041.

This is a PDF file of an unedited manuscript that has been accepted for publication. As a service to our customers we are providing this early version of the manuscript. The manuscript will undergo copyediting, typesetting, and review of the resulting proof before it is published in its final form. Please note that during the production process errors may be discovered which could affect the content, and all legal disclaimers that apply to the journal pertain.

An Improved Static-Analytic Apparatus for Vapor-Liquid Equilibrium (PT_{xy}) Measurement Using Modified In-situ Samplers

Fan Zhang^{a,b}, Pascal Théveneau^a, Elise El Ahmar^a, Xavier Canet^b, Chien-Bin Soo^b,

Christophe Coquelet^{a,*}

^aMINES ParisTech, PSL - Research University, CTP - Centre Thermodynamique des Procédés, 35 rue Saint Honoré, 77300 Fontainebleau, France

^bPROCESSIUM, CEI 3, 62 Boulevard Niels Bohr, 69603 Villeurbanne, France

Abstract

An improved apparatus based on the static-analytic method for reliable vapor-liquid equilibrium (VLE) data measurement is presented in this work. It has been applied to investigate systems containing organic sulfur compounds. New sampling mechanisms were combined with ROLSITM capillary samplers to achieve on-line sampling for both vapor and liquid phases in a pressure range between 0.1 and 10 bar. Phase samples were directly sent to a gas chromatograph for composition analysis. The equipment was tested against other commonly used experimental methods in this pressure range on the (*n*-butane + ethanol) and (diethyl sulfide + ethanol) systems. The obtained data were correlated by Wilson model and compared with existing data. The improved apparatus has shown comparable performances to existing methods, while showing some advantages such as complete PT_{xy} phase measurements and less product consumption. After the validation step, additional VLE data for binary systems of interest, (diethyl sulfide + *n*-butane) and (1-pentanethiol + 1-pentanol), were reported and modeled in this work.

Key words: in-situ sampling, ROLSITM capillary sampler, gas chromatography analysis, low pressure, organic sulfur compounds

1. Introduction

Accurate knowledge of phase diagrams is of great importance in chemical engineering. It serves as the basis for separation process design (e.g. distillation and extraction) and ensures a proper selection of equipment and operating conditions. Experimental data and thermodynamic models are part and parcel of understanding phase behavior and thermodynamic properties; hence high-quality experimental data and reliable techniques continue to be highly regarded in industries [1].

Organic sulfur compounds, such as thiols and sulfides, are commonly found as impurities in crude oils, as well as in products from petroleum refining processes [2]. As the regulations for sulfur contents in market fuels are getting stricter [3], the sulfur removal processes need to evolve accordingly. However, experimental data for organic sulfur compounds are rare, especially for those having relatively long carbon chains ($> 3C$). We assume there is a lack of adapted techniques for Vapor-Liquid Equilibrium (VLE) measurement using analytic methods like gas chromatography. Moreover, dealing with sulfur component, which can be toxic, in a laboratory scale needs appropriate apparatus design to ensure operation security without losing data accuracy. The suggested solution consists in using equipment based on the “static-analytic” method.

In this work, we focus on the development of new equipment for experimental acquisition of VLE data at low pressure. In effect, most experimental data for systems containing organic sulfur compounds ($> 3C$) are within low pressure (from sub-atmospheric pressures to several bar). In this pressure region, our literature survey has revealed that the most commonly used technique is the total-pressure measurement method [4,5], which is also known as the “static-synthetic” method. By measuring the equilibrium pressure of a multi-phase mixture of known global composition at isothermal conditions, one may deduce phase

compositions by using material balance [6]. Without phase sampling, the static-synthetic method requires thermodynamic models to perform material balance calculations. The chosen thermodynamic models therefore may influence the experimental results. At pressures around or under 1 bar, glass dynamic circulation stills (also known as ebulliometers) are widely used. They are able to provide complete VLE data ($PTxy$). Some authors suggested using stainless steel [7–10], instead of glass, to extend the applications up to several bar. Although these apparatuses have shown promising results, they hold some typical limitations of circulation stills, such as large system volume and condenser cooling duty. They act as feasible alternatives only in selected applications.

The “static-analytic” method consists of taking samples from all coexisting phases in an equilibrium cell, and analyzing sample compositions [6]. Thus, both vapor and liquid phase compositions are experimentally determined. Compared with the static-synthetic method, the static-analytic method does not require data reduction via thermodynamic models. In-situ sampling from a closed cell dispenses with phase circulation and condensation which are vital for a circulation still. Thus, chemical consumption and operation risk may be reduced by the static-analytic method. For these reasons, the static-analytic method seems more suitable for VLE measurements involving organic sulfur compounds.

Since the publication of the first static-analytic apparatus designed in our laboratory [11], development has been made to extend its application. Laugier et al. [12] used a variable volume cell in order to measure simultaneously VLE data and volumetric properties. Baba-Ahmed et al. [13] suggested an apparatus for measurements under cryogenic conditions (down to 77 K). The equilibrium cell was thereafter redesigned by Houssin-Agbomson et al. [14]. Guilbot et al. [15] described in detail the Rapid On-Line Sampler-Injector (ROLSITM) allowing in-situ withdrawals of microliters of phase samples. It has been used for numerous measurements afterwards [16–19]. The sampling can be achieved through the ROLSITM

sampler, as long as the cell pressure exceeds that of the carrier gas for gas chromatograph (GC), usually around 3 bar. At pressures lower than 3 bar, the lack of pressure driving force would make this sampling mechanism fail, as the carrier gas would enter the cell and contaminate the contents. Consequently, measurements under 3 bar have always posed sampling difficulties for our laboratory.

In order to develop an experimental apparatus adapting to organic sulfur compounds and to cover the pressure gap under 3 bar, we have proposed new sampling mechanisms for ROLSITM capillary sampler to allow in-situ phase sampling at pressures lower than 3 bar. The improved static-analytic apparatus is capable of measuring PT_{xy} equilibrium data from 0.1 up to 10 bar. In this work, the newly developed apparatus is presented while highlighting the modified samplers. The latter is validated by measuring VLE data of two well-documented binary systems (*n*-butane + ethanol) and (diethyl sulfide + ethanol). The obtained data are correlated through the Wilson equation [20] with Soave–Redlich–Kwong equation of state (SRK EoS) [21] for vapor phase, and compared with those determined by other experimental methods in the open literature. After the validation step, additional VLE data are reported for two binary systems containing organic sulfur compounds: (diethyl sulfide + *n*-butane) and (1-pentanethiol + 1-pentanol). The newly measured data are also correlated by Wilson model.

2. Description of the apparatus

The “*classic*” static-analytic apparatus described by Laugier and Richon [11] acts as the starting point for our development. The essential configuration of the classic static-analytic type apparatus is retained. The equilibrium cell consists of a sapphire tube tightly sealed by two titanium flanges at the top and bottom. Its internal volume is approximately 100 mL. Three valves connected to the cell permit loading, discharging, degassing and evacuation

operations. The equilibrium cell is immersed in a thermo-regulated liquid bath (LAUDA Proline RP 3530 C). A variable-speed stirrer inside the cell accelerates the mass transfer between phases and reduces the time needed to achieve equilibrium. In order to ensure accurate temperature measurements in the equilibrium cell and to check for thermal gradients, temperature is measured at the top and bottom flanges through two 100 Ω platinum resistance thermometer probes. Pressures are measured by three pressure transducers (General Electric, model UNIK 5000) of which the maximum absolute pressures are 0.35 bar, 1 bar and 10 bar, respectively. The pressure transducers are maintained at a constant temperature (353 K throughout this work) by means of a PID regulator (WEST instrument, model 6100). Both temperature and pressure signals from the sensors are transmitted to a data acquisition unit (Agilent 34972A) which is linked to a computer for record. Sample analysis is carried out by a gas chromatograph (Perichrom, model PR-2100) equipped with a thermal conductivity detector (TCD). Peak integration and analysis is performed using the data acquisition software WINILAB III (Perichrom, France).

Two ROLSITM capillary samplers are installed to perform in-situ sampling. The samples are firstly sent to a thermo-regulated transfer line and then swept to the GC by carrier gas for composition analysis. To carry out phase sampling at pressures lower than 3 bar, we made the following adaptations, respectively for liquid and vapor phases.

For liquid phase, a small cylindrical chamber (PVT) is drilled in the bottom flange. The chamber is equipped with a piston and connected to the equilibrium cell through a capillary (see Figure 1). A small amount of liquid phase can be withdrawn via suction, and then compressed after the valve V_4 is closed, in order to generate the pressure driving force required to sample through the liquid ROLSITM sampler (LS). The pressure exerted for compression can be regulated via a manometer. After taking the desired number of samples, the remaining liquid in the PVT chamber is pushed back into the equilibrium cell. The

assembly of PVT chamber and ROLSI™ capillary sampler is the subject of a patent recently submitted [22].

[Figure 1]

Vapor phase sampling under 3 bar is achieved by using a 6-port sample injection valve (6PV). The 6-port valve is connected to the transfer line, and is thermo-regulated. Prior to sampling, it allows the vacuum pump to evacuate the sample loop (SL, dashed line in Figure 1). A vapor phase sample is then taken through the vapor ROLSI™ sampler (VS) via vacuum and swept to GC by switching to carrier gas circulation. The 6-port valve is not used for vapor phase sampling, when the cell pressure is above the pressure of carrier gas.

The main innovative modification in this improved apparatus, compared with the classic version, is to isolate a small amount of liquid phase in the PVT chamber and compress it for sampling. Piston movement is carefully controlled to ensure that the isolated liquid is representative of that in the equilibrium cell. No significant impact on equilibrium has been perceived after withdrawing this quantity from the liquid phase. Considering sample volume (usually less than 5 μL per sample) taken by ROLSI™ capillary sampler for analysis, the compressed liquid allows a sufficient number of samples to obtain a representative mean value for the composition, as well as check for repeatability. After sampling, the remaining liquid can be flushed back to the equilibrium cell without disturbing the established equilibrium. Further testing was conducted to validate the performance of the liquid sampling system. Under some equilibrium conditions, after filling once the PVT chamber and obtaining repeatable liquid phase compositions, we emptied the PVT chamber and repeated the liquid sampling procedure to take more samples. Despite refilling the PVT chamber with independent charges, we could still ensure liquid composition repeatability within $\pm 1\%$.

The main advantage of compressing the liquid phase, instead of sampling via vacuum as for the vapor phase, is the possibility to control the generated pressure driving force. As liquid is denser and more viscous than vapor, the pressure driving force may be insufficient for sampling via vacuum, especially under sub-atmospheric conditions. With the proposed liquid sampling system, viscous fluids such as amines can be easily dealt with.

3. Experimental

The validation of the improved apparatus is conducted by carrying out isothermal VLE measurements for two well-documented binary systems. The selected test systems, (*n*-butane + ethanol) and (diethyl sulfide + ethanol), were previously measured using a variety of different methods (see Table 1), so that the performance of the improved apparatus can be compared with existing methods. We focus mainly on the pressure range in which the classic static-analytic type apparatus is unable to perform sampling, i.e. lower than 3 bar.

[Table 1]

After the validation step, two binary systems of interest, (diethyl sulfide + *n*-butane) and (1-pentanethiol + 1-pentanol), are investigated. Isothermal data for the system (diethyl sulfide + *n*-butane) were previously measured by the static-synthetic method at 317.60 K [25]. This data set serves as a double check on our apparatus.

All the details concerning the chemicals used are presented in Table 2.

[Table 2]

3.1. Calibration

The temperature probes were carefully calibrated against a 25 Ω reference platinum resistance thermometer (TINLEY Precision Instruments). The reference thermometer was

calibrated by the Laboratoire National d'Essais (Paris) based on the 1990 International Temperature Scale (ITS 90). The three pressure transducers were calibrated against a digital pressure balance (Desgranges & Huot 24610).

The following GC columns were used to analyze the compositions of samples:

- HayeSep T, 100/120 mesh (length 1.6 m, diameter 2 mm, from Restek France) maintained at 413 K for the system (*n*-butane + ethanol)
- Porapak Q, 50 / 80 mesh (length 2.1 m, diameter 2 mm, from Restek France) maintained at 493 K for the systems (diethyl sulfide + ethanol) and (diethyl sulfide + *n*-butane)
- 10% Squalane, 80 / 100 mesh (length 2 m, diameter 2 mm, from Restek France) maintained at 423 K for the system (1-pentanethiol + 1-pentanol)

The TCD of gas chromatograph was repeatedly calibrated by injecting known amounts of each pure compound via a syringe into the injector.

The uncertainty estimation procedure is described in Appendix. Both measurement repeatability and calibration uncertainty have been considered. We report all the expanded uncertainties (U , coverage factor $k = 2$) for experimental data in Section 5.

3.2. Experimental procedures

The equilibrium cell and its loading lines were evacuated. About 15 mL of the less volatile component was introduced via a syringe. The liquid was degassed by periodically removing vapor phase through an overhead valve, while heating to the desired temperature. Meanwhile, adequate stirring was maintained inside the cell. The lighter component was then loaded via a thermal press to a pressure level corresponding to the pressure of the first measurement. Phase equilibrium was assumed to be achieved while temperature and pressure

readings stabilized for at least 30 minutes. For each equilibrium condition, at least 5 samples of both vapor and liquid phases were withdrawn and analyzed to ensure composition repeatability within $\pm 1\%$. The lighter component was then further introduced to measure the next equilibrium condition.

4. Data correlation

The γ - ϕ approach was considered for VLE data correlation. The Wilson equation [20] was chosen for liquid phase, while the SRK equation of state [21] was used for vapor phase. The pure compound properties used for modeling are presented in Table 3. All calculation was performed with the software Simulis Thermodynamics [26].

[Table 3]

Wilson interaction parameters (λ_{12} and λ_{21}) were fitted on the data obtained through our improved apparatus, by minimizing the objective function (OF):

$$OF = \sum \left(\frac{|P_{exp} - P_{cal}|}{P_{exp}} + \frac{|y_{exp} - y_{cal}|}{y_{exp}} \right) \quad (1)$$

The fitted Wilson interaction parameters are presented with the experimental data in the next section.

5. Results and discussion

5.1. Test systems

5.1.1. *n*-Butane + ethanol

The experimental data and correlation results for the system (*n*-butane + ethanol) are given in Table 4. The isothermal Pxy diagram is plotted in Figure 2, along with existing data.

The obtained results have also been expressed in terms of relative volatility $\alpha_{1/2}$, an important index for the design of a distillation column [29], and presented versus liquid phase composition in Figure 2.

[Table 4]

[Figure 2]

As observed from Figure 2, good agreement is observed between the measurements of this work and those performed by other methods, for both liquid and vapor compositions. As the main objective is to validate the sampling mechanisms below 3 bar, few points at higher pressures were measured. However, with the interaction parameters fitted on the data measured in this work, the entire isotherm (as well as the azeotropic point) is well represented (see Table 5).

[Table 5]

The proposed apparatus is able to cover the entire pressure range of the test system, from 0.4 to 5 bar. Although the static-synthetic measurements conducted by Holderbaum et al. [23] were capable of covering the same pressure range, experimental vapor phase compositions were not available. Soo et al. [19] used a classic static-analytic apparatus similar to that of Valtz et al. [16], and yielded vapor phase information. However, without the proposed modifications at the time, the measurements were restricted to pressures between 4.0 and 5.0 bar. The improved apparatus has shown the ability to provide the desired PT_{xy} data for the entire pressure range. Prior to the new measurements, at least two apparatuses were necessary to cover the entire pressure range, while essential information, such as the vapor phase compositions, would still be missing at pressures lower than 4 bar.

Rapidity of data acquisition using the proposed apparatus is comparable to that of the classic version. Measurements were conducted under continuous mode by consecutive loading of the lighter component after each equilibrium condition. Only the static-analytic approach outputs data at a faster rate, but it does not provide experimental information on vapor phase and requires proper selection of thermodynamic models.

5.1.2. Diethyl sulfide + ethanol system

The experimental data and correlation results for the system (diethyl sulfide + ethanol) are given in Table 6. The isothermal P_{xy} diagram and the relative volatility versus liquid composition are plotted in Figure 3, along with the existing data.

[Table 6]

[Figure 3]

The entire pressure range of 0.5 – 0.9 bar can be covered by both experimental methods. One observes, from Figure 3, that the data measured by both methods are in good agreement. The maximum pressure azeotrope has been identified. The differences between the calculated data and the experimental ones are generally close to the experimental uncertainties (see Table 6). The deviations of the calculated data from our data and those given by Ref. [24] are very similar (see Table 5). Our apparatus has shown comparable performance with circulation still at sub-atmospheric pressures, while the lower consumption of chemicals is an advantage for measurements with toxic or expensive components. Moreover, it is easier to handle systems containing gaseous or viscous components in a static cell than in a circulation still.

5.2. Newly investigated systems

5.2.1. Diethyl sulfide + *n*-butane system

The experimental data and correlation results for the system (diethyl sulfide + *n*-butane) at 317.62 K and 343.13 K are given in Table 7. The isothermal P_{xy} diagram is plotted in Figure 4, along with the existing data.

[Table 7]

[Figure 4]

Measurements were performed not only under the pressure of GC carrier gas (usually around 3 bar), but also extended up to 7.3 bar. The data measured by the proposed apparatus at 317.62 K are in good agreement with those obtained by Dell'Era et al. [25] at 317.60 K. The deviations of the calculated data from both data sets are also similar (see Table 5). We notice that Dell'Era et al. [25] provided PT_{xy} data measured by the static-synthetic method, instead of PT_x data as the authors of Ref. [4,5] did. However, the vapor phase compositions are computed (through SRK EoS [21]) rather than experimentally determined. In practice, the vapor phase volume needs to be minimized so that the global composition is close to the liquid phase composition, as pointed out by Dicko et al. [30].

Additional data were measured at 343.14 K and correlated by Wilson model with satisfactory results (see Table 5).

5.2.2. 1-Pentanethiol + 1-pentanol system

The experimental data and correlation results for the system (1-pentanethiol + 1-pentanol) at 372.75 K and 392.72 K are given in Table 8. The isothermal P_{xy} diagram is plotted in Figure 5, along with the existing data.

[Table 8]

[Figure 5]

To the best of our knowledge, no VLE data for the system (1-pentanethiol + 1-pentanol) were available in the open literature. The new PT_{xy} data are well correlated by Wilson model. The deviations are generally similar to those obtained for the other 3 systems (see Table 5). The maximum pressure azeotropes are captured at both temperatures. They are computed through Wilson model: $P = 0.468$ bar, $x_I = 0.831$ at 372.75 K and $P = 0.882$ bar, $x_I = 0.771$ at 392.72 K.

6. Conclusion

In this work, we presented a new apparatus capable of providing reliable and complete VLE data (PT_{xy}) from 0.1 up to 10 bar. It was applied to investigate systems containing organic sulfur compounds (especially those having over 3 carbons). The apparatus is based on the static-analytic method. Starting from a classic configuration, improvements have been made for both vapor and liquid samplers to permit in-situ sampling and GC analysis even at pressures lower than that of the carrier gas. Continuous operation ensured that data can be measured in a relatively short time.

The improved apparatus was tested against two binary systems: (*n*-butane + ethanol) and (diethyl sulfide + ethanol). The experimental results were correlated by Wilson model and compared with the available data. Good agreements have been observed between the obtained data and those measured through commonly used experimental methods. In the past, a complete phase diagram of these two systems would have required at least two measurement

techniques, while the comparison showed that the new apparatus alone is sufficient to yield the complete phase diagram.

Once the apparatus was validated, two systems of interest were then investigated: (diethyl sulfide + *n*-butane) and (1-pentanethiol + 1-pentanol). The obtained data were correlated by Wilson model, leading to satisfactory results.

The improved apparatus addresses an identified lack of VLE data for systems containing organic sulfur compounds. However, its application can be extended to other systems within the same pressure range (under 10 bar). With the growing demands for accurate VLE data in this range, the presented apparatus provides a solution to industries seeking process design and optimization using experimental thermodynamics. Additional experimental data measured through the new apparatus will be published in future papers.

Appendix: Uncertainty Estimation

To estimate the uncertainties in temperature, pressure and composition, we have followed the guidelines of NIST [31]. Both measurement repeatability and calibration uncertainties are taken into account.

The mean of a series of independent observations can be considered as a good approximation to the value of the measurand (θ). The standard uncertainty (u) due to this calculation, also known as “repeatability”, is determined by the recommended expression:

$$u_{rep}(\theta) = \sqrt{\frac{1}{N(N-1)} \sum_{i=1}^N (\theta_i - \theta_{avg})^2} \quad (\text{A.1})$$

where the subscript *rep* denotes repeatability, N is the number of observations, θ_i is the result of i th observation, and θ_{avg} is the mean of N observations.

The standard uncertainty arising from calibration (u_{calib}) is estimated by considering two sources: reference (u_{ref}) and polynomial regression (u_{reg}) between the displayed values and those given by the reference. The former is provided by the reference manufacturer, while the latter is evaluated statistically. The measurement result θ is calculated through the polynomial of which the coefficients are “uncertain” and dependent on each other. The standard uncertainty $u_{reg}(\theta)$ can be estimated through the law of propagation of uncertainty which is based on a first-order Taylor series approximation of the polynomial:

$$u_{reg}(\theta) = \sqrt{\sum_{i=0}^K \left(\frac{\partial f}{\partial a_i}\right)^2 u^2(a_i) + 2 \sum_{i=0}^{K-1} \sum_{j=i+1}^K \left(\frac{\partial f}{\partial a_i}\right) \left(\frac{\partial f}{\partial a_j}\right) u(a_i, a_j)} \quad (\text{A.2})$$

where f is the polynomial of degree K , a_i is the i th order coefficient of the polynomial f , $u(a_i)$ is the standard uncertainty of the coefficient a_i , and $u(a_i, a_j)$ is the covariance associated with a_i and a_j . All $u(a_i)$ and $u(a_i, a_j)$ can be estimated by calculating the covariance matrix from the calibration data.

The combined standard uncertainty of the measurement result θ , designated by $u_c(\theta)$, is obtained from:

$$u_c(\theta) = \sqrt{u_{rep}^2(\theta) + u_{calib}^2(\theta)} = \sqrt{u_{rep}^2(\theta) + u_{ref}^2(\theta) + u_{reg}^2(\theta)} \quad (\text{A.3})$$

The combined standard uncertainty u_c is then multiplied by $k = 2$, leading to the overall expanded uncertainty (U) with a level of confidence of approximately 95%.

Acknowledgment

Processium, represented by Dr. Pascal Rousseaux, is gratefully acknowledged for its financial support. The technical supports from Mr. A. Valtz and Mr. H. Legendre are also appreciated.

Nomenclature

List of Symbols

a = coefficient of the polynomial f (in Appendix)

f = polynomial correlating the displayed values and those given by the reference during calibration step (in Appendix)

k = coverage factor for uncertainty estimation

K = degree of the polynomial f (in Appendix)

N = number of independent observations (in Appendix)

P = pressure (bar)

T = temperature (K)

u = standard uncertainty (see Appendix)

$u(a_i, a_j)$ = covariance associated with a_i and a_j (in Appendix)

U = overall expanded uncertainty

v = liquid molar volume

x = mole fraction in liquid phase

y = mole fraction in vapor phase

Greek letters

$\alpha_{1/2}$ = relative volatility of component (1) versus component (2)

γ = activity coefficient

θ = measurand (in Appendix)

λ = Wilson interaction parameter

φ = fugacity coefficient

ω = acentric factor

Subscripts

1 = relative to component (1) of binary system

2 = relative to component (2) of binary system

c = relative to combined uncertainty (in Appendix)

avg = relative to arithmetic mean (in Appendix)

cr = relative to critical point

cal = relative to calculated data

calib = relative to calibration (in Appendix)

exp = relative to experimental data

ref = relative to reference (in Appendix)

reg = relative to polynomial regression (in Appendix)

rep = relative to measurement repeatability (in Appendix)

References

- [1] E. Hendriks, G.M. Kontogeorgis, R. Dohrn, J.-C. de Hemptinne, I.G. Economou, L.F. Žilnik, V. Vesovic, *Ind. Eng. Chem. Res.* 49 (2010) 11131–11141. doi:10.1021/ie101231b.
- [2] J.H. Gary, G.E. Handwerk, M.J. Kaiser, *Petroleum Refining: Technology and Economics*, 5th ed., CRC Press Taylor & Francis Group, Boca Raton, London, New York, 2007.
- [3] European Parliament, Directive 2003/17/EC, (2003).
- [4] R.E. Gibbs, H.C. Van Ness, *Ind. Eng. Chem. Fundam.* 11 (1972) 410–413. doi:10.1021/i160043a022.
- [5] B. Kolbe, J. Gmehling, *Fluid Phase Equilib.* 23 (1985) 213–226. doi:10.1016/0378-3812(85)90007-X.
- [6] J.M.S. Fonseca, R. Dohrn, S. Peper, *Fluid Phase Equilib.* 300 (2011) 1–69. doi:10.1016/j.fluid.2010.09.017.
- [7] X. Huang, S. Xia, P. Ma, S. Song, B. Ma, *J. Chem. Eng. Data.* 53 (2008) 252–255. doi:10.1021/je7005665.
- [8] P. Susial, A. Sosa-Rosario, R. Rios-Santana, *J. Chem. Eng. Data.* 55 (2010) 5701–5706. doi:10.1021/je100614r.
- [9] R. Chen, L. Zhong, C. Xu, *J. Chem. Eng. Data.* 57 (2012) 155–165. doi:10.1021/je200921u.
- [10] P. Reddy, J.D. Raal, D. Ramjugernath, *Fluid Phase Equilib.* 358 (2013) 121–130. doi:10.1016/j.fluid.2013.07.044.
- [11] S. Laugier, D. Richon, *Sci. Instrum.* 57 (1986) 469–472. doi:10.1063/1.1138909.
- [12] S. Laugier, D. Richon, H. Renon, *Fluid Phase Equilib.* 54 (1990) 19–34. doi:10.1016/0378-3812(90)85067-K.
- [13] A. Baba-Ahmed, P. Guilbot, D. Richon, *Fluid Phase Equilib.* 166 (1999) 225–236. doi:10.1016/S0378-3812(99)00294-0.
- [14] D. Houssin-Agbomson, C. Coquelet, D. Richon, P. Arpentinier, *Cryogenics.* 50 (2010) 248–256. doi:10.1016/j.cryogenics.2010.01.014.
- [15] P. Guilbot, A. Valtz, H. Legendre, D. Richon, *Analisis.* 28 (2000) 426–431. doi:10.1051/analisis:2000128.
- [16] A. Valtz, C. Coquelet, A. Baba-Ahmed, D. Richon, *Fluid Phase Equilib.* 202 (2002) 29–47. doi:10.1016/S0378-3812(02)00056-0.

- [17] C. Coquelet, A. Chareton, A. Valtz, A. Baba-Ahmed, D. Richon, *J. Chem. Eng. Data.* 48 (2003) 317–323. doi:10.1021/je020115d.
- [18] P. Guilbot, K. Fischer, A. Valtz, P. Théveneau, A. Baba-Ahmed, D. Richon, *Fluid Phase Equilib.* 260 (2007) 49–59. doi:10.1016/j.fluid.2007.07.013.
- [19] C.-B. Soo, E. El Ahmar, C. Coquelet, D. Ramjugernath, D. Richon, *Fluid Phase Equilib.* 286 (2009) 79–87. doi:10.1016/j.fluid.2009.08.007.
- [20] G.M. Wilson, *J. Am. Chem. Soc.* 86 (1964) 127–130. doi:10.1021/ja01056a002.
- [21] G. Soave, *Chem. Eng. Sci.* 27 (1972) 1197–1203. doi:10.1016/0009-2509(72)80096-4.
- [22] Armines, Dispositif pour prélever des micro-échantillons d'un fluide à l'état liquide contenu dans un conteneur. French Patent Application No. 1460309, 2014.
- [23] T. Holderbaum, A. Utzig, J. Gmehling, *Fluid Phase Equilib.* 63 (1991) 219–226. doi:10.1016/0378-3812(91)80032-Q.
- [24] E. Sapei, P. Uusi-Kyyny, K.I. Keskinen, J.-P. Pokki, V. Alopaeus, *Fluid Phase Equilib.* 301 (2011) 200–205. doi:10.1016/j.fluid.2010.11.026.
- [25] C. Dell'Era, J.-P. Pokki, P. Uusi-Kyyny, M. Pakkanen, V. Alopaeus, *Fluid Phase Equilib.* 291 (2010) 180–187. doi:10.1016/j.fluid.2010.01.006.
- [26] Simulis Thermodynamics version 2.0.4, ProSim SA, Labège, France.
- [27] B. Poling, J. Prausnitz, J.O. Connell, *The Properties of Gases and Liquids*, McGraw Hill Professional, 2000.
- [28] T.E. Daubert, R.P. Danner, H.M. Sibul, C.C. Stebbins, *DIPPR Data compilation of pure compound properties*, Design Institute for Physical Property Data, AIChE, New York, NY, 1993.
- [29] R.H. Perry, D.W. Green, J.O. Maloney, *Perry's Chemical Engineers' Handbook 7th Edition*, McGraw-Hill, USA, 1997.
- [30] M. Dicko, C. Coquelet, P. Theveneau, P. Mougin, *J Chem Eng Data.* 57 (2012) 1534–1543. doi:10.1021/je300111m.
- [31] B.N. Taylor, C.E. Kuyatt, *Guidelines for evaluating and expressing the uncertainty of NIST measurement results*, National Institute of Standards and Technology, Gaithersburg, MD, 1994.

Table 1. Test systems measured via the proposed apparatus and previously performed measurements

Table 2 Chemical sample

Table 3 Critical pressure (P_{cr}), critical temperature (T_{cr}), acentric factor (ω) and liquid molar volume (v) at 298.15 K of the involved compounds

Table 4. Experimental data and correlation results for the *n*-butane (1) + ethanol (2) system measured via the proposed apparatus

Table 5. Deviations of calculated data from experimental data for the four binary systems measured by the proposed apparatus and by other methods

Table 6. Experimental data and correlation results for the diethyl sulfide (1) + ethanol (2) system measured via the proposed apparatus

Table 7. Experimental data and correlation results for the diethyl sulfide (1) + *n*-butane (2) system measured via the proposed apparatus

Table 8. Experimental data and correlation results for the 1-pentanethiol (1) + 1-pentanol (2) system measured via the proposed apparatus

ACCEPTED MANUSCRIPT

Table 1

| Improved apparatus | | | Previous experimental methods | | | |
|----------------------------|---------|-----------|-------------------------------|-----------|-----------|------|
| Test System | T (K) | P (bar) | Method | Data type | P (bar) | Ref. |
| <i>n</i> -butane + ethanol | 323.22 | 0.4 – 5.0 | Static-synthetic | PT_x | 1.3 – 5.0 | [23] |
| | | | Classic static-analytic | PT_{xy} | 4.0 – 5.0 | [19] |
| diethyl sulfide + ethanol | 343.15 | 0.5 – 0.9 | Circulation still | PT_{xy} | 0.5 – 0.9 | [24] |

Table 2

| Chemical name | Source | Initial purity | Purification method | Final purity | Analysis method |
|------------------|------------------|----------------|---------------------|--------------|-----------------|
| <i>n</i> -Butane | Air Liquide | 0.995 vol. | None | -- | SM ^a |
| Ethanol | Fischer Chemical | 0.9999 mol. | None | -- | SM |
| Diethyl sulfide | Sigma-Aldrich | 0.98 mol. | None | -- | SM |
| 1-Pentanol | Sigma-Aldrich | 0.99 mol. | None | -- | SM |
| 1-Pentanethiol | Sigma-Aldrich | 0.98 mol. | None | -- | SM |

^a Supplier method

Table 3

| Compound | <i>n</i> -butane | Ethanol | Diethyl sulfide | 1-Pentanol | 1-Pentanethiol |
|------------------------------|------------------|---------|-----------------|------------|----------------|
| P_{cr}^a (bar) | 37.96 | 61.37 | 39.60 | 39.09 | 34.70 |
| T_{cr}^a (K) | 425.12 | 513.92 | 557.00 | 588.15 | 598.00 |
| ω^a | 0.200 | 0.649 | 0.295 | 0.579 | 0.321 |
| v^b (cm ³ /mol) | 101.40 | 58.63 | 108.36 | 108.54 | 124.53 |

^a from Ref. [27]^b calculated through DIPPR correlation [28]

Table 4

| $x_{1\text{ exp}}$ | $U(x_1)$ | Nb. of samples | $y_{1\text{ exp}}$ | $U(y_1)$ | Nb. of samples | P_{exp}^a (bar) | Δy_1^b | ΔP^c (bar) |
|---|----------|----------------|--------------------|----------|----------------|-----------------------------|----------------|-----------------------|
| $T = 323.22\text{ K}^d$; $\lambda_{12} = 1414.3\text{ J/mol}$ & $\lambda_{21} = 8536.9\text{ J/mol}$ | | | | | | | | |
| 0 | -- | -- | 0 | -- | -- | 0.294 | -- | -- |
| -- ^e | -- | -- | 0.272 | 0.009 | 6 | 0.413 | -- | -- |
| -- ^e | -- | -- | 0.423 | 0.008 | 6 | 0.526 | -- | -- |
| 0.014 | 0.001 | 9 | 0.568 | 0.009 | 5 | 0.702 | -0.019 | -0.015 |
| 0.032 | 0.001 | 11 | 0.743 | 0.007 | 5 | 1.205 | -0.014 | -0.016 |
| 0.053 | 0.002 | 8 | 0.819 | 0.005 | 5 | 1.713 | -0.009 | 0.000 |
| 0.078 | 0.003 | 9 | 0.863 | 0.004 | 6 | 2.208 | -0.003 | 0.009 |
| 0.109 | 0.004 | 10 | 0.892 | 0.003 | 5 | 2.718 | 0.000 | 0.019 |
| 0.205 | 0.006 | 7 | 0.924 | 0.003 | 6 | 3.720 | 0.001 | 0.031 |
| 0.323 | 0.008 | 9 | 0.938 | 0.002 | 6 | 4.320 | 0.002 | 0.014 |
| 0.544 | 0.009 | 8 | 0.943 | 0.002 | 6 | 4.734 | -0.002 | -0.020 |

^a $U(P) = 0.002\text{ bar}$ for $P < 1\text{ bar}$; $U(P) = 0.003\text{ bar}$ for $P > 1\text{ bar}$

^b $\Delta y_1 = y_{1\text{ exp}} - y_{1\text{ cal}}$

^c $\Delta P = P_{\text{exp}} - P_{\text{cal}}$

^d $U(T) = 0.02\text{ K}$

^e Liquid phase compositions were below the detection threshold of the TCD.

Table 5

| Binary system | T (K) | AAD y_1^a | AARD P^b (%) | Ref. |
|--|---------|-------------|----------------|------------------------|
| <i>n</i> -butane (1) + ethanol (2) | 323.22 | 0.006 | 0.8 | this work ^c |
| | 323.25 | 0.004 | 1.4 | [19] |
| | 323.75 | -- | 0.4 | [23] |
| diethyl sulfide (1) + ethanol (2) | 343.13 | 0.006 | 0.7 | this work ^c |
| | 343.15 | 0.003 | 0.4 | [24] |
| diethyl sulfide (1) + <i>n</i> -butane (2) | 317.62 | 0.004 | 1.2 | this work ^c |
| | 317.60 | 0.001 | 1.0 | [25] |
| | 343.14 | 0.002 | 0.5 | this work ^c |
| 1-pentanethiol (1) + 1-pentanol (2) | 372.75 | 0.007 | 0.5 | this work ^c |
| | 392.72 | 0.005 | 0.3 | this work ^c |

^a Average absolute deviation:

$$AAD y_1 = (1/N) \sum_{i=1}^N (|y_{1 \text{ exp } i} - y_{1 \text{ cal } i}|)$$

^b Average absolute relative deviation:

$$AARD P (\%) = (100/N) \sum_{i=1}^N (|P_{\text{exp } i} - P_{\text{cal } i}|/P_{\text{exp } i})$$

^c Data set used for parameter fitting

Table 6

| $x_{1\text{ exp}}$ | $U(x_1)$ | Nb. of samples | $y_{1\text{ exp}}$ | $U(y_1)$ | Nb. of samples | P_{exp}^a (bar) | Δy_1 | ΔP (bar) |
|--|----------|----------------|--------------------|----------|----------------|--------------------------|--------------|------------------|
| $T = 343.13\text{ K}^b$; $\lambda_{12} = 497.6\text{ J/mol}$ & $\lambda_{21} = 4778.8\text{ J/mol}$ | | | | | | | | |
| 0 | -- | -- | 0 | -- | -- | 0.720 | -- | -- |
| 0.027 | 0.001 | 12 | 0.069 | 0.002 | 6 | 0.753 | 0.001 | -0.004 |
| 0.063 | 0.002 | 6 | 0.139 | 0.004 | 5 | 0.798 | 0.000 | 0.005 |
| 0.110 | 0.003 | 6 | 0.204 | 0.006 | 6 | 0.825 | -0.001 | -0.001 |
| 0.148 | 0.004 | 9 | 0.244 | 0.006 | 6 | 0.848 | 0.000 | 0.004 |
| 0.243 | 0.006 | 6 | 0.317 | 0.007 | 6 | 0.871 | 0.003 | -0.001 |
| 0.321 | 0.007 | 6 | 0.362 | 0.008 | 6 | 0.878 | 0.009 | -0.002 |
| 0.368 | 0.008 | 6 | 0.375 | 0.008 | 6 | 0.883 | 0.003 | 0.001 |
| 0.444 | 0.008 | 5 | 0.407 | 0.008 | 6 | 0.877 | 0.008 | -0.003 |
| 0.649 | 0.008 | 6 | 0.483 | 0.008 | 5 | 0.847 | 0.016 | -0.005 |
| 0.761 | 0.006 | 5 | 0.541 | 0.009 | 5 | 0.811 | 0.022 | -0.002 |
| 0.902 | 0.003 | 10 | 0.660 | 0.008 | 5 | 0.707 | 0.002 | 0.009 |
| 0.964 | 0.002 | 10 | 0.811 | 0.005 | 5 | 0.608 | -0.002 | 0.017 |
| 0.979 | 0.001 | 10 | 0.885 | 0.004 | 5 | 0.563 | 0.006 | 0.009 |
| 1 | -- | -- | 1 | -- | -- | 0.497 | -- | -- |

^a $U(P) = 0.002\text{ bar}$ ^b $U(T) = 0.03\text{ K}$

Table 7

| $x_{1\text{ exp}}$ | $U(x_1)$ | Nb. of samples | $y_{1\text{ exp}}$ | $U(y_1)$ | Nb. of samples | P_{exp}^a (bar) | Δy_1 | ΔP (bar) |
|--|----------|----------------|--------------------|----------|----------------|--------------------------|--------------|------------------|
| $T = 317.62\text{ K}^b$; $\lambda_{12} = 346.0\text{ J/mol}$ & $\lambda_{21} = 1053.6\text{ J/mol}$ | | | | | | | | |
| 0.090 | 0.003 | 6 | 0.009 | 0.001 | 5 | 3.909 | 0.001 | 0.006 |
| 0.268 | 0.007 | 6 | 0.024 | 0.001 | 5 | 3.233 | 0.000 | 0.005 |
| 0.461 | 0.009 | 5 | 0.042 | 0.002 | 5 | 2.551 | -0.002 | 0.000 |
| 0.678 | 0.008 | 5 | 0.079 | 0.003 | 5 | 1.719 | -0.003 | -0.040 |
| 0.847 | 0.005 | 5 | 0.157 | 0.005 | 5 | 0.991 | -0.007 | -0.036 |
| 0.973 | 0.001 | 6 | 0.507 | 0.009 | 5 | 0.354 | -0.013 | -0.003 |
| 1 | -- | -- | 1 | -- | -- | 0.190 | -- | -- |
| $T = 343.14\text{ K}^b$; $\lambda_{12} = 304.0\text{ J/mol}$ & $\lambda_{21} = 994.4\text{ J/mol}$ | | | | | | | | |
| 0.088 | 0.005 | 6 | 0.014 | 0.001 | 5 | 7.323 | 0.002 | -0.044 |
| 0.225 | 0.006 | 5 | 0.030 | 0.001 | 5 | 6.308 | 0.001 | -0.022 |
| 0.383 | 0.008 | 5 | 0.051 | 0.002 | 6 | 5.206 | -0.001 | -0.033 |
| 0.608 | 0.008 | 5 | 0.096 | 0.003 | 5 | 3.717 | -0.002 | 0.000 |
| 0.805 | 0.006 | 5 | 0.186 | 0.006 | 5 | 2.231 | -0.006 | -0.033 |
| 0.969 | 0.002 | 6 | 0.604 | 0.009 | 5 | 0.806 | 0.001 | 0.001 |
| 1 | -- | -- | 1 | -- | -- | 0.497 | -- | -- |

^a $U(P) = 0.002$ bar for $P < 1$ bar; $U(P) = 0.003$ bar for $P > 1$ bar

^b $U(T) = 0.03$ K

Table 8

| $x_{1\text{ exp}}$ | $U(x_1)$ | Nb. of samples | $y_{1\text{ exp}}$ | $U(y_1)$ | Nb. of samples | P_{exp}^a (bar) | Δy_1 | ΔP (bar) |
|--|----------|----------------|--------------------|----------|----------------|--------------------------|--------------|------------------|
| $T = 372.75\text{ K}^b$; $\lambda_{12} = 384.2\text{ J/mol}$ & $\lambda_{21} = 2970.6\text{ J/mol}$ | | | | | | | | |
| 0 | -- | -- | 0 | -- | -- | 0.243 | -- | -- |
| 0.056 | 0.002 | 6 | 0.197 | 0.006 | 5 | 0.283 | 0.011 | -0.001 |
| 0.130 | 0.004 | 8 | 0.351 | 0.008 | 6 | 0.323 | 0.010 | -0.003 |
| 0.203 | 0.006 | 7 | 0.452 | 0.009 | 5 | 0.357 | 0.010 | -0.003 |
| 0.321 | 0.008 | 7 | 0.560 | 0.009 | 6 | 0.401 | 0.009 | 0.000 |
| 0.543 | 0.009 | 6 | 0.685 | 0.008 | 5 | 0.442 | 0.005 | -0.004 |
| 0.838 | 0.005 | 6 | 0.834 | 0.005 | 5 | 0.466 | -0.002 | -0.002 |
| 0.942 | 0.002 | 6 | 0.925 | 0.002 | 5 | 0.461 | 0.000 | -0.001 |
| 1 | -- | -- | 1 | -- | -- | 0.451 | -- | -- |
| $T = 392.72\text{ K}^b$; $\lambda_{12} = 243.6\text{ J/mol}$ & $\lambda_{21} = 2868.5\text{ J/mol}$ | | | | | | | | |
| 0 | -- | -- | 0 | -- | -- | 0.534 | -- | -- |
| 0.052 | 0.002 | 6 | 0.147 | 0.004 | 5 | 0.591 | 0.007 | -0.004 |
| 0.123 | 0.004 | 6 | 0.280 | 0.007 | 6 | 0.658 | 0.004 | -0.004 |
| 0.209 | 0.006 | 6 | 0.392 | 0.008 | 6 | 0.723 | 0.000 | -0.002 |
| 0.390 | 0.008 | 7 | 0.550 | 0.009 | 6 | 0.814 | 0.003 | 0.000 |
| 0.584 | 0.008 | 6 | 0.670 | 0.008 | 7 | 0.861 | 0.008 | -0.003 |
| 0.828 | 0.005 | 10 | 0.819 | 0.005 | 6 | 0.882 | 0.008 | 0.002 |
| 0.865 | 0.004 | 7 | 0.849 | 0.005 | 5 | 0.877 | 0.008 | 0.001 |
| 0.940 | 0.002 | 9 | 0.920 | 0.003 | 5 | 0.859 | 0.004 | 0.001 |
| 1 | -- | -- | 1 | -- | -- | 0.831 | -- | -- |

^a $U(P) = 0.002\text{ bar}$ ^b $U(T) = 0.03\text{ K}$

Figure 1. Flow diagram of the proposed apparatus. 6PV: 6-port sample injection valve; C: carrier gas; EC: equilibrium cell; GC: gas chromatograph; LS: liquid ROLSITM sampler; MS: magnetic stirrer; PP: platinum resistance thermometer probe; PT: pressure transducer; PVT: PVT chamber for liquid phase sampling; SL: Sample Loop; V_i: valve; VP: vacuum pump; VS: vapor ROLSITM sampler; VSM: variable speed motor.

Figure 2. (A) Isothermal Pxy diagram for the VLE of the *n*-butane (1) + ethanol (2) system. (B) Relative volatility $\alpha_{1/2}$ plotted versus x_1 . (○) Data measured in this work at 323.22 K; (Δ) Data from Holderbaum et al. [23] measured by static-synthetic method at 323.75 K; (□) Data from Soo et al. [19] measured by classic static-analytic method at 323.25 K; (—) calculated by Wilson model. Error bars: expanded uncertainties calculated from composition uncertainties ($k = 2$).

Figure 3. (A) Isothermal Pxy diagram for the VLE of the diethyl sulfide (1) + ethanol (2) system. (B) Relative volatility $\alpha_{1/2}$ plotted versus x_1 . (○,●) Data measured in this work at 343.13 K; (□,■) Data from Sapei et al. [24] measured by circulation still at 333.15 K; (—) calculated by Wilson model. Error bars: expanded uncertainties calculated from composition uncertainties ($k = 2$).

Figure 4. Isothermal Pxy diagram for the VLE of the diethyl sulfide (1) + *n*-butane (2) system. (○) Data measured in this work at 317.62 K and 343.14 K; (□) Data from Dell'Era et al. [25] measured by the static-synthetic method at 317.60 K (vapor phase compositions were calculated through SRK EoS [21]); (—) calculated by Wilson model.

Figure 5. Isothermal P_{xy} diagram for the VLE of the 1-pentanethiol (1) + 1-pentanol (2) system. (\circ, \bullet) Data measured in this work at 372.75 K and 392.72 K; (—) calculated by Wilson model.

ACCEPTED MANUSCRIPT

Figure 1

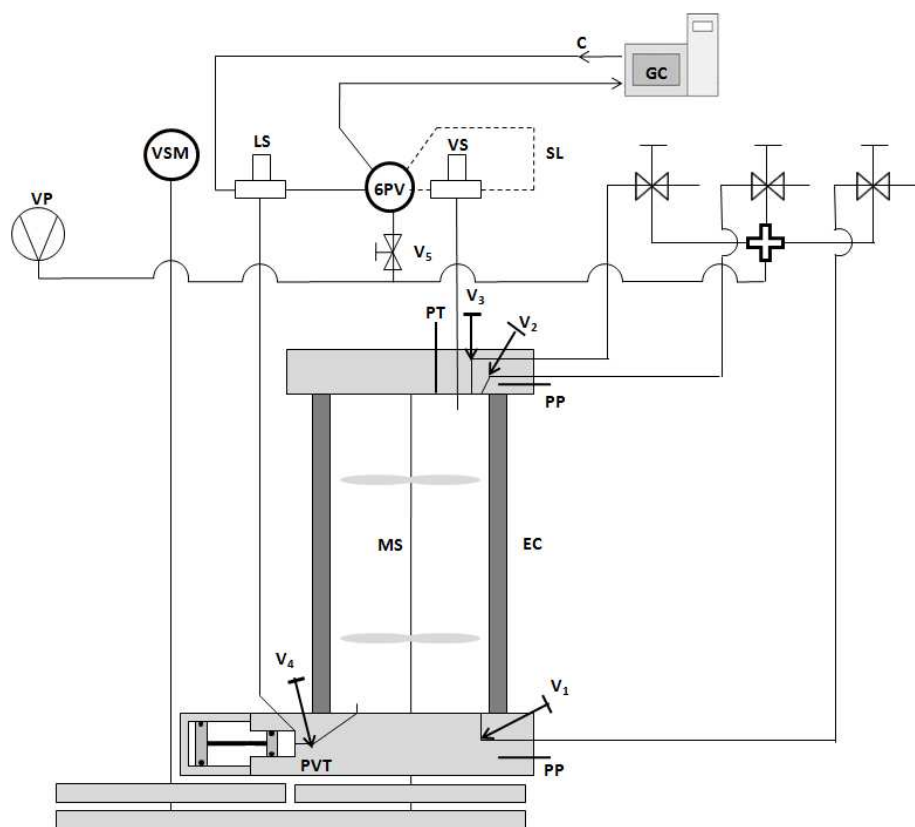


Figure 2

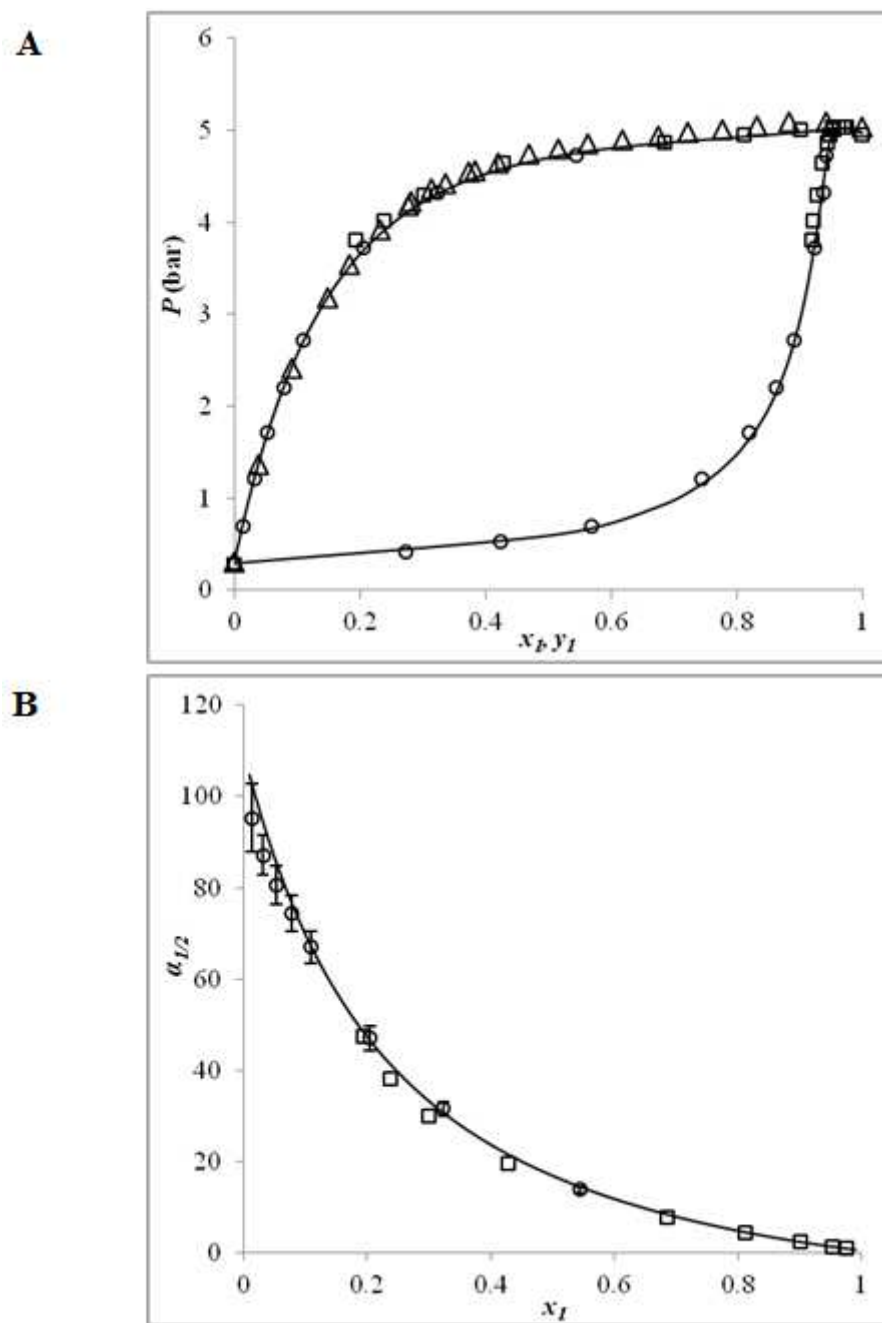


Figure 3

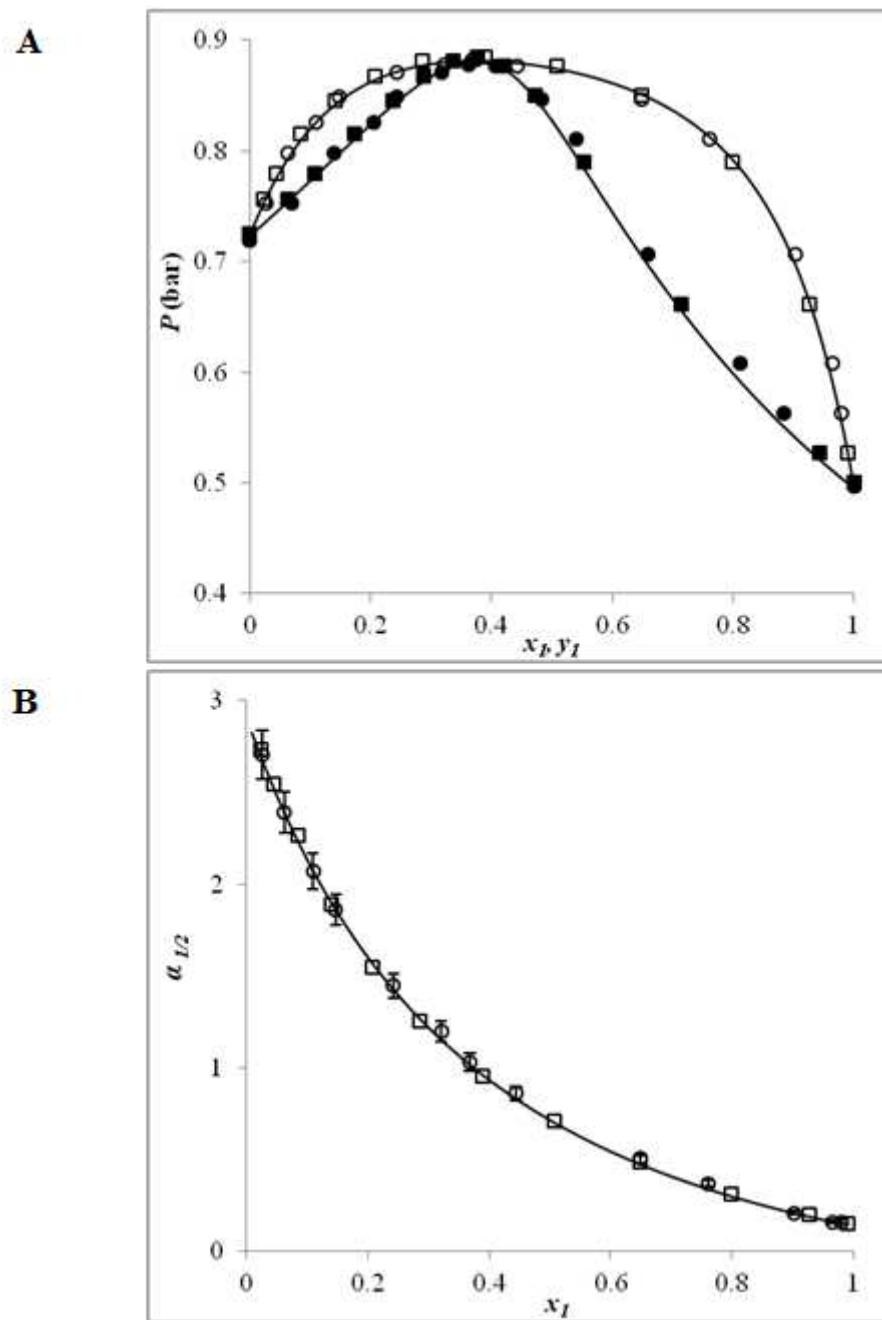


Figure 4

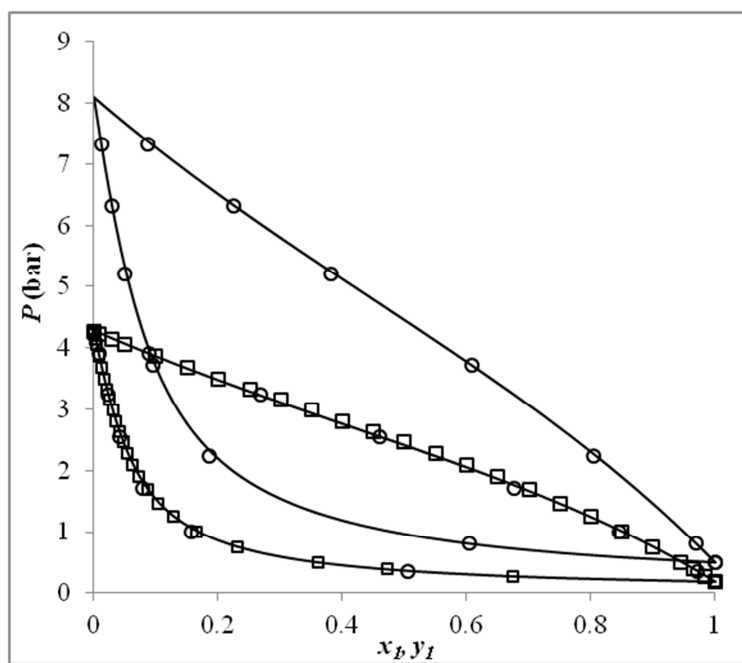


Figure 5

